



OPEN ACCESS

EDITED BY

Xinping Hu,
Texas A&M University Corpus Christi,
United States

REVIEWED BY

Jonathan Erez,
Hebrew University of Jerusalem, Israel
Tali Mass,
University of Haifa, Israel

*CORRESPONDENCE

Alexander A. Venn
avenn@centrescientifique.mc

SPECIALTY SECTION

This article was submitted to
Coral Reef Research,
a section of the journal
Frontiers in Marine Science

RECEIVED 20 June 2022

ACCEPTED 09 September 2022

PUBLISHED 23 September 2022

CITATION

Venn AA, Tambutté E, Comeau S and
Tambutté S (2022) Proton gradients
across the coral calcifying cell layer:
Effects of light, ocean acidification and
carbonate chemistry.
Front. Mar. Sci. 9:973908.
doi: 10.3389/fmars.2022.973908

COPYRIGHT

© 2022 Venn, Tambutté, Comeau and
Tambutté. This is an open-access article
distributed under the terms of the
[Creative Commons Attribution License
\(CC BY\)](https://creativecommons.org/licenses/by/4.0/). The use, distribution or
reproduction in other forums is
permitted, provided the original
author(s) and the copyright owner(s)
are credited and that the original
publication in this journal is cited, in
accordance with accepted academic
practice. No use, distribution or
reproduction is permitted which does
not comply with these terms.

Proton gradients across the coral calcifying cell layer: Effects of light, ocean acidification and carbonate chemistry

Alexander A. Venn^{1*}, Eric Tambutté¹, Steeve Comeau²
and Sylvie Tambutté¹

¹Marine Biology Department, Centre Scientifique de Monaco, Monaco, Monaco, ²Sorbonne Université, CNRS-INSU, Laboratoire d'Océanographie de Villefranche, Villefranche-sur-mer, France

In corals, pH regulation of the extracellular calcifying medium (ECM) by the calcifying cell layer is a crucial step in the calcification process and is potentially important to influencing how corals respond to ocean acidification. Here, we analyzed the growing edge of the reef coral *Stylophora pistillata* to make the first characterization of the proton gradient across the coral calcifying epithelium. At seawater pH 8 we found that while the calcifying epithelium elevates pH in the ECM on its apical side above that of seawater, pH on its basal side in the mesoglea is markedly lower, highlighting that the calcifying cells are exposed to a microenvironment distinct from the external environment. Coral symbiont photosynthesis elevates pH in the mesoglea, but experimental ocean acidification and decreased seawater inorganic carbon concentration lead to large declines in mesoglea pH relative to the ECM, which is maintained relatively stable. Together, our results indicate that the coral calcifying epithelium is functionally polarized and that environmental variation impacts pH_{ECM} regulation through its effects on the basal side of the calcifying cells.

KEYWORDS

pH regulation, biomineralization, scleractinian, physiology, climate-change

Introduction

Reef-building, scleractinian corals are among the most ecologically and biogeochemically important of the ocean's calcifying organisms. They are responsible for the creation of vast edifices of CaCO₃ that serve as a habitat for thousands of species (Sheppard et al., 2017). The coral calcification mechanism is a complex biologically controlled process which is currently the subject of intense research due to the vulnerability of corals to climate change and the wide-use of geochemical signatures in

coral skeletons as proxy-indicators of environmental variation (Tambutté et al., 2011; Drake et al., 2020; Fietzke and Wall, 2022; Gilbert et al., 2022).

Recent research indicates that the first steps of coral calcification begin in the calcifying (calicoblastic) cells where ACC precursors initially form in vesicles and are released into the extracellular calcifying medium (ECM) where the skeleton grows (Mass et al., 2017; Schmidt et al., 2022). The calicoblastic cells also transport Ca^{2+} ions and dissolved inorganic carbon (DIC) into the ECM and regulate its pH to values that are higher than the surrounding seawater (Venn et al., 2011; Sevilgen et al., 2019). pH regulation of the ECM (pH_{ECM}) by the calicoblastic cells creates CaCO_3 saturation states that favor the growth of the skeleton and removes protons that are generated during the mineralization process (McCulloch et al., 2012; Venn et al., 2013; Cyronak et al., 2016; Sevilgen et al., 2019; Sun et al., 2020).

Despite the crucial role of pH regulation in the physiology driving coral calcification, mechanistic understanding of how the calicoblastic cells control pH_{ECM} is poor. Lacking from our understanding is a functional perspective of how the calicoblastic epithelium transports acidity away from the ECM, although molecular studies have proposed a number of membrane-bound transporters that may be involved (Zoccola et al., 2004; Zoccola et al., 2015; Capasso et al., 2021). Indeed, most previous studies on coral pH regulation focus solely on ECM measurements and little attention has been paid to the physiology of the calcifying cells themselves or their microenvironment. Values of pH_{ECM} tend to be presented in the literature next to seawater pH values (Ries, 2011; McCulloch et al., 2012; Venn et al., 2013) despite multiple tissue layers lying in between the ECM and the external environment. Indeed, when viewed as a section through the tissue (Tambutté et al., 2011), the apical side of the calicoblastic cells faces the ECM and their basal side faces a connective tissue termed the mesoglea. The mesoglea is largely acellular, apart from scattered amoebocytes, and studies on its composition in anthozoans have shown that it is a highly hydrated material containing 86% water, made up of a two-phase system of collagen fibers embedded in a matrix of proteins and polysaccharides (Gosline, 1971; Parisi et al., 2021). The pH of the mesoglea in corals has never been determined and this layer is generally overlooked in studies on ion transport/pH regulation, despite being in immediate contact with the calcifying cells. The mesoglea is itself spatially separated from seawater by the aboral endoderm, the extracellular space of the coelenteron lumen, the oral endoderm containing most of the symbiotic dinoflagellates and the oral ectoderm which faces the external seawater (Tambutté et al., 2011).

Understanding how calicoblastic cells regulate pH in the context of their apical and basal microenvironments within the organism has profound implications for our understanding of how and why coral calcification responds to environmental variation. It is well known that ocean acidification (decreases

in seawater pH due to oceanic uptake of man-made CO_2) drives down pH in the ECM of many coral species (Wall et al., 2016; Comeau et al., 2019; Venn et al., 2019; Comeau et al., 2022), but a clear physiological understanding of how and why pH_{ECM} and intracellular pH (pH_i) of the calicoblastic epithelium responds to ocean acidification is lacking. Other changes in seawater carbonate chemistry also modulate pH_{ECM} including variation in seawater dissolved inorganic carbon concentration [DIC] (Comeau et al., 2017; McCulloch et al., 2017) but the links between seawater carbonate chemistry and pH_{ECM} are not fully understood. Irradiance is another factor that has been observed to change pH_{ECM} and although the process presumably involves photosynthetic activity of the symbiotic dinoflagellates in the endoderm layer, the reason why photosynthesis affects pH_{ECM} regulation by the calicoblastic cells is far from clear. The limits of current understanding in this field are reflected in the widespread use of numerical models that simulate the response of coral calcification to environmental change but treat many aspects of coral physiology as a black box. For example, in simulating the dynamics of ECM chemistry, the ECM is frequently assumed to exchange (mix) directly with seawater or the coelenteron (Adkins et al., 2003; Sinclair and Risk, 2006; Gagnon et al., 2012; Hohn and Merico, 2012; Venn et al., 2013; Ohno et al., 2017a; Guo, 2019; Gagnon et al., 2021), despite the existence of intervening cell layers and extracellular microenvironments such as the mesoglea.

The objective of the current study was to provide new insight into how the coral calcifying cell layer regulates pH of the ECM by characterizing its transcellular proton gradient. To achieve this, we determined pH in the mesoglea on the basal side of the calcifying cells, in addition to intracellular pH of the calicoblastic epithelium and pH_{ECM} on its apical side. Furthermore, we conducted laboratory experiments to investigate how the proton gradient across the coral calcifying epithelium responded to three environmental factors: light/darkness, ocean acidification and modified seawater dissolved inorganic carbon (DIC) concentrations and total alkalinity (TA). The investigation was conducted on the widely used model scleractinian coral *Stylophora pistillata*, by *in vivo* confocal analysis of the growing edge of coral colonies cultivated on glass coverslips (Muscatine et al., 1997; Raz-Bahat et al., 2006; Venn et al., 2011). This approach allows visualization of the calcifying epithelium and has previously facilitated significant advances in our understanding of biomineralization in both juvenile and adult corals in recent years (Tambutté et al., 2012; Mass et al., 2017; Ohno et al., 2017b; Neder et al., 2019). Our findings revealed that the calicoblastic epithelium is functionally polarized, elevating pH in the ECM on its apical side but decreasing pH on its basal side, causing the mesoglea to be at markedly different pH than seawater. Experiments with light and dark exposure, lowered seawater pH and modified DIC (and TA) revealed how all three environmental factors cause pH variation in the mesoglea, whereas pH remained relatively stable in the ECM.

Material and methods

Experimental design

The study was performed on the model scleractinian coral *Stylophora pistillata* at the Centre Scientifique de Monaco between 2014 and 2017. Three experiments were carried out in this period, in which pH was measured in the mesoglea, calcicoblastic epithelium and ECM of coral microcolonies. In the first experiment corals, were analyzed in seawater at pH 8 (shown in Figure 1). pH data from this experiment (mesoglea, calcicoblastic epithelium and ECM) have not been published previously. In the second experiment (shown in Figure 2) seawater was acidified to pH 7.8, 7.4 and 7.2 by bubbling with CO₂. In this experiment, pH values from the mesoglea have not been published previously, but pH in the calcicoblastic epithelium and ECM in the same corals were reported previously in Venn et al. (2019). In the third experiment (shown in Figure 3), the dissolved inorganic carbon concentration [DIC] of seawater was manipulated. In this experiment, pH values from the mesoglea were not published previously, but pH in the calcicoblastic epithelium and ECM in the same corals were reported previously in Comeau et al. (2017). In the second and third experiments, consideration of the new mesoglea pH values next to previously published pH values of the calcicoblastic epithelium and ECM allowed determination of transepithelial proton gradients in these experiments.

Experimental treatments

Microcolonies of *S. pistillata* were grown laterally on glass coverslips in long-term coral culture facilities supplied with flowing seawater from the Mediterranean Sea (exchange rate 2% h⁻¹), total scale pH (pH_T) 8, salinity 38, with temperature maintained at 25°C, under an irradiance of 175 μmol photons m⁻² s⁻¹ on a 12h: 12 h light: dark cycle (Venn et al., 2011; Comeau et al., 2017; Venn et al., 2019; Venn et al., 2020). Corals were fed daily with frozen rotifers and twice weekly with live *Artemia salina* nauplii. When coral microcolonies were approximately 1 cm² in surface area they were transferred to one of the three experimental set ups described below.

For the first experiment (results shown in Figure 1), samples (n=6) were maintained in two 20-L aquaria supplied with Mediterranean seawater (exchange rate 60% per hour), with flow provided by aquarium pumps, pH maintained at pH 8.02 ± 0.01 (mean ± SD) at the same salinity, temperature and under the same irradiance conditions described above for culture facilities.

For the seawater acidification experiments, microcolonies were maintained for one week in eight acidification treatment aquaria (20-L) prior to analysis. Aquaria consisted of four pH treatments (two aquaria per treatment) maintained at pH_T 7.2,

7.4, 7.8 and 8.0. Seawater pH and carbonate chemistry was controlled by a custom-made CO₂ and CO₂ free-air bubbling and monitoring system (Enleo, Monaco). These aquarium treatments are identical to those reported in Venn et al., 2019 (Venn et al., 2019), although the aquarium at pH 8.0 was referred to as the seawater pH 8.1 treatment in (Venn et al., 2019) (Venn et al., 2019). Temperature was maintained at 25 ± 1°C, with seawater renewal rate of 60% per hour and irradiance provided at 175 μmol photons m⁻² s⁻¹ on a 12h: 12 h light: dark cycle. Submersible pumps (EHEIM 3000) ensured high water circulation in each aquarium. Five samples were exposed to each pH treatment (n=5) with the microcolonies split between the two aquaria at each pH level (two in one aquarium, three in the other). Further details of seawater acidification treatments and full seawater carbonate chemistry are given in the supplementary materials (Supplementary Table 1) and also previously reported (Venn et al., 2019).

In the seawater [DIC] experiments, microcolonies were maintained in eight 20-L tanks for 15 days. Aquaria consisted of four [DIC] treatments (two aquaria per treatment) with pH maintained constant at ~7.9, while [DIC] (and Total Alkalinity (TA)) was manipulated to cover a range of [DIC] from ~800 to 2900 μmol kg⁻¹. For ease of reference these treatments are referred to by their DIC concentration as “very low” (~800 μmol kg⁻¹), “low” (~1500 μmol kg⁻¹), “ambient” (~2200 μmol kg⁻¹) and “high” (~2900 μmol kg⁻¹) [DIC]. Six microcolonies (n=6) were exposed to each [DIC] treatment (3 per aquarium). Temperature was maintained at 25 ± 1°C, with seawater renewal rate of 60% per hour and irradiance provided at 175 μmol photons m⁻² s⁻¹ on a 12h: 12 h light: dark cycle. Submersible pumps (EHEIM 3000) ensured high water circulation in each aquarium.

Further methodological details of DIC manipulation experiments and the seawater carbonate chemistry parameters are reported in Supplementary Table 2 and previously (Comeau et al., 2017).

pH imaging by confocal microscopy

pH was measured in the mesoglea, extracellular calcifying medium (pH_{ECM}), calcicoblastic epithelium (pH_i) by inverted confocal microscopy (Leica SP5, Germany) and the pH sensitive dyes SNARF-1 (cell impermeant) and SNARF-1 AM (cell permeant) (ThermoFisher Scientific) according to methods reported in (Comeau et al., 2017; Venn et al., 2019). The analysis was carried out in cell culture perfusion chambers (POC-R2, PeCon, Germany) mounted on a temperature-controlled stage-insert on the confocal microscope. Irradiance was provided at 175 μmol photons m⁻² s⁻¹ and temperature maintained at 25°C with perfusion rates at a 50% per minute renewal rate of the volume of liquid in the chamber.

For measurement of pH in the mesoglea and ECM, samples were first perfused with seawater drawn from the relevant

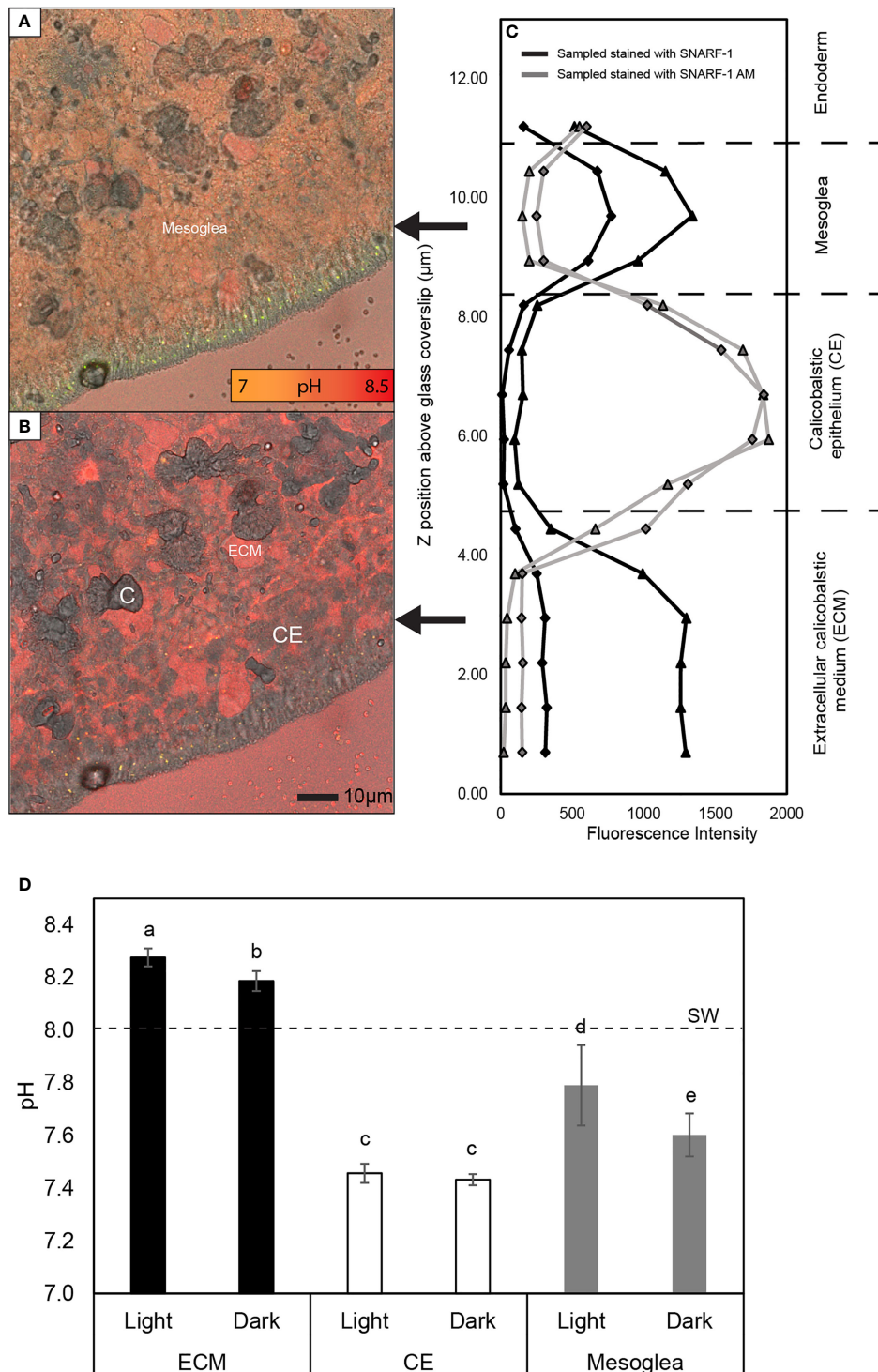


FIGURE 1 Analysis of the pH gradient across the calcifying epithelium of *S. pistillata*. (A, B) Examples of merged confocal and transmitted light images taken in the mesoglea (A) and the extracellular calcifying medium (ECM) (B) at 9 and 2 μm above the glass coverslip in a microcolony stained with cell impermeant SNARF-1. C = crystals and CE = calciblastic epithelium. (C) Example of fluorescence data obtained in separate Z stacks showing elevated fluorescence of cell impermeant SNARF-1 in the ECM and mesoglea, and of cell permeant SNARF-1 AM in the CE. Triangle and diamond symbols indicate fluorescence captured at 585 ± 10 and 640 ± 10 nm respectively. (D) Mean pH \pm SD of the ECM, calciblastic epithelium and mesoglea in light and darkness at seawater pH 8. SW= seawater pH. Letters above bars indicate significantly different groups determined by *post hoc* pairwise comparisons using Mann Whitney U tests.

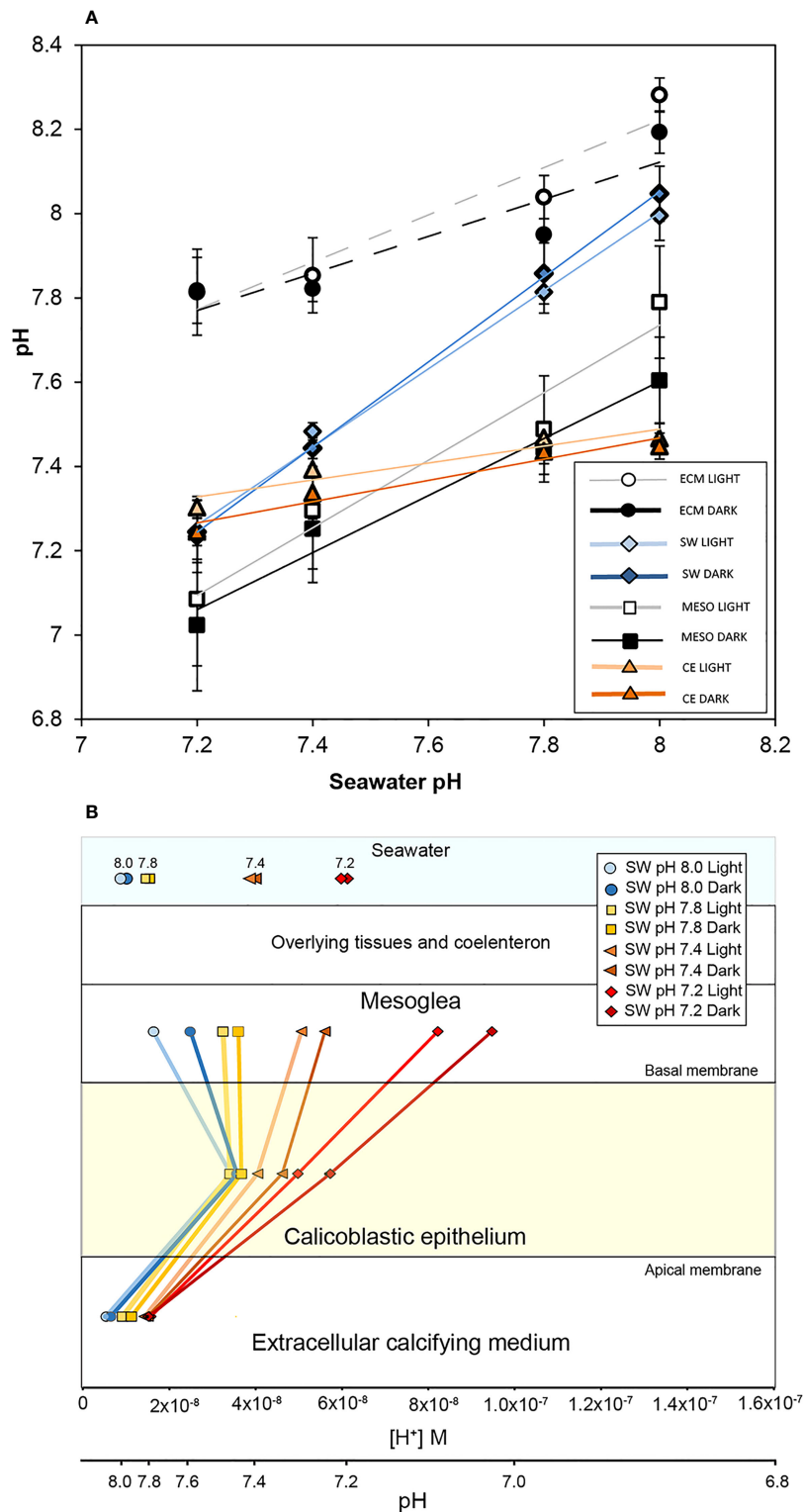


FIGURE 2
 The effect of seawater acidification in light and darkness on the pH gradient across the calcifying epithelium of *S. pistillata*. **(A)** pH (means \pm SD) in the mesoglea (MESO), seawater surrounding the corals in the perfusion chamber (SW), the extracellular calcifying medium (ECM) and the calcicoblastic epithelium (CE). ECM and CE values taken from Venn et al. (2019). A linear regression is drawn for each data set to display the trend. **(B)** Mean pH values from panel (A) plotted against parallel $[H^+]$ and pH scales to illustrate the proton gradient across the CE.

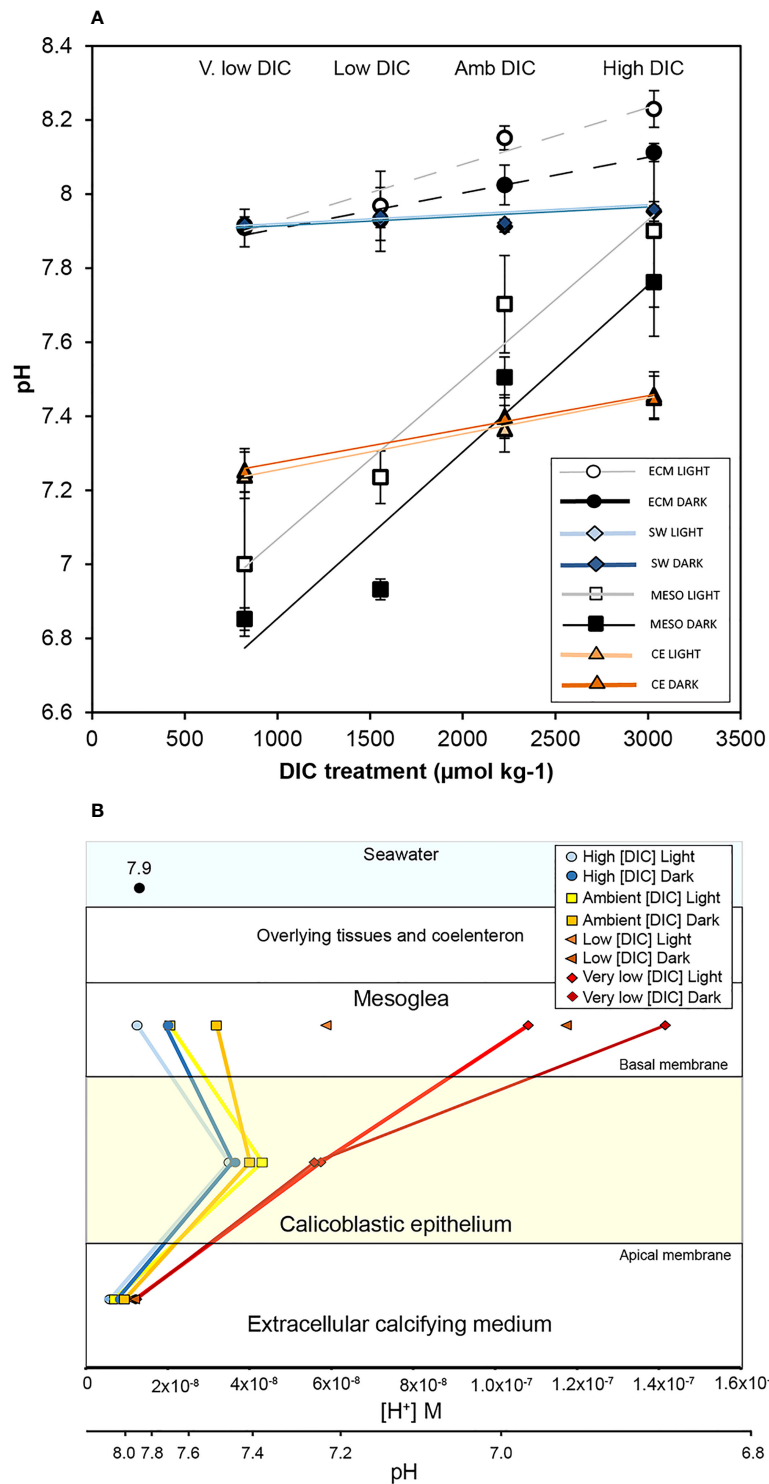


FIGURE 3

The influence of seawater dissolved inorganic carbon concentration [DIC] and in light and darkness on the pH gradient across the calcifying epithelium of *S. pistillata*. (A) pH (means ± SD) in the mesoglea (MESO), seawater surrounding the corals in the perfusion chamber (SW), the extracellular calcifying medium (ECM) and the calcicoblastic epithelium (CE). ECM and CE values taken from (Comeau et al., 2017). A linear regression is drawn for each data set to display the trend. (B) Mean pH values from panel (A) plotted on parallel [H⁺] and pH scales to illustrate the proton gradient across the CE. The pH level of seawater (pH 7.9) is indicated in the seawater compartment. Low [DIC] treatment pH_i values in the CE are not shown as they were not measured in Comeau et al. (2017).

experimental treatment for 20 min in light or darkness, before being perfused with a seawater solution of 45 μM cell-impermeable SNARF-1 for a 5 min loading period in light or darkness. Perfusion continued for a further 10 min in light or darkness during which repeated pH measurements were taken in the coral and the surrounding seawater.

For pH_i in the calcicoblastic epithelium, samples were first perfused with seawater drawn from the relevant experimental treatment for 20 min in light or darkness, then perfused with 10 μM cell-permeable SNARF-1 AM for a 10 min loading period, before making repeated measurements in the coral during 10 min period of perfusion with seawater in light or darkness.

For pH measurements in the mesoglea, ECM and cells, Confocal Z stacks of optical sections were obtained at the growing edge of microcolonies (Venn et al., 2011), from the surface of the glass coverslip upwards through the tissue over a vertical distance of at least 12 μm . Imaging was carried out at 40X magnification by excitation at 543 nm at 30% laser intensity, and fluorescence captured in two channels at emission wavelengths of 585 ± 10 nm and 640 ± 10 nm. Post-processing of images involved acquiring SNARF-1 fluorescence of each channel from digital regions of interest (ROI) drawn in each optical section of the Z stacks.

pH calibration

Calibration of the SNARF-1 ratio to pH in the mesoglea was carried out as follows. Coral microcolonies were perfused with buffered artificial seawater (ASW) containing SNARF-1 at pH 6.5, 7.0, 7.5, 8.0 and 8.5 (National Bureau of Standards (NBS)) for a 10 min period. ASW was made up with 490mM NaCl, 10 mM CaCl_2 , 27mM MgCl_2 , 29 mM MgSO_4 , 2 mM NaHCO_3 and 10 mM KCl in dH_2O (Benazet-Tambutte 1996) and contained 25mM Tricine or PIPES. Confocal optical sections were taken in the mesoglea in both light and darkness at each pH level to obtain the fluorescence ratio of SNARF-1 from the two emission capture channels (see above). These data were plotted against pH and a calibration curve was produced (supplementary Figure S1).

The mesoglea SNARF-1 fluorescence signal was related to pH by the following equation:

$$\text{pH} = \text{pK}_A - \log \left[\frac{R - R_B/R_A}{X} \times \frac{F_{A(\lambda_2)}}{F_{A(\lambda_1)}} \right]$$

where (F) is fluorescence intensity measured at 640 nm (λ_2) and the subscripts A and B represent the limiting values at the acidic and basic end points of the titration respectively (i.e. pH 6 and 8.5) (Venn et al., 2009).

We validated our *in vivo* calibration of the mesoglea in *S. pistillata* by analyzing the SNARF-1 ratio/pH relationship directly in isolated mesoglea with the adjoining cell layers removed. As the mesoglea is thin and difficult to dissect in *S. pistillata*, we used the anemone *A. viridis*. Tentacles were removed from anemones using

dissection scissors, opened longitudinally, and forceps used to scrap away both ectoderm and endoderm cell layers (Bénazet-Tambutte et al., 1996). A 1cm^2 piece was cut from the remaining mesoglea, rinsed three times in filtered seawater and incubated in the desired ASW buffer solution containing SNARF-1 for 10 min. The piece of mesoglea was then mounted between a glass slide and coverslip and confocal analyses were performed in the same manner as for *S. pistillata* by acquiring Z stacks upwards from the coverslip through the mesoglea. Analysis of the SNARF-1 ratio in isolated mesoglea dissected from *A. viridis* strongly agreed with the ratios we obtained in *S. pistillata* over the range of our calibration (Supplementary Figure S1). The agreement of our ratios in *S. pistillata* and isolated mesoglea ruled out the possibility that our *in vivo* mesoglea calibration in *S. pistillata* was spurious due to biological activity (e.g. respiration and ion transport) by the adjoining cell layers or due to attenuation of the SNARF-1 signal by the calcicoblastic epithelium.

Calibration procedures for the ECM and calcicoblastic cells have been described previously (Venn et al., 2011) to total scale pH (pH_T) and National Bureau of Standards (NBS) pH scale respectively.

Collagen imaging

For imaging of collagen using Col-F (ImmunoChemistry Technologies), stock solutions were prepared at 20mM in DMSO. Microcolonies were incubated in filtered seawater containing a working solution of 20 μM Col-F at 25°C for 10 min in perfusion chambers (POC-R2). Confocal images were obtained at surface of the glass coverslip upwards through the tissue over a vertical distance of 15- 20 μm . Imaging was performed at 40 X magnification, with excitation at 488 nm at 50% laser intensity, and fluorescence captured at emission wavelengths of 515 ± 15 nm.

Data analysis

Confocal images were analyzed using LASX software v. 3.5.2.18 (Leica). Statistical analysis was carried out using SPSS software v. 26 (IBM). Non parametric or parametric tests were carried out following Shapiro-wilks tests and Levene's tests for normality and homogeneity of variance respectively.

Results

Imaging pH across the coral calcifying epithelium at ambient seawater pH 8

Coral colonies were analyzed by mounting corals in a perfusion chamber fitted on an inverted confocal microscope

and perfusing corals with seawater and fluorescent indicator dyes. Sequences of images were acquired in vertical 'Z-stacks' beginning below the coral tissue at the level of the glass coverslip, moving upwards through the extracellular calcifying medium (ECM) on the apical side of the calciblastic epithelium, the calciblastic cells themselves and into the extracellular microenvironment on its basal side i.e. into the mesoglea (Figures 1A, B). In colonies perfused with the cell impermeant form of carboxysemaphthorhodafleur-1 (SNARF-1) (which stains extracellular spaces), fluorescence was detected in the first optical sections of the Z stack taken in the ECM but decreased sharply as the Z-stack passed through the calciblastic cells (which exclude the impermeable form of the dye). The fluorescence then increased again once the Z stack passed through the basal membrane of the cells into the extracellular environment of the mesoglea (Figure 1C).

Z-stacks of microcolonies stained with the cell permeant form of the dye, SNARF-1 AM, which concentrates in the intracellular environment, produced the inverse pattern to Z-stacks with cell impermeable SNARF-1, displaying low fluorescence in the extracellular environment of the ECM, but elevated fluorescence in the middle of the Z stack in the calciblastic epithelium, and low fluorescence again in the mesoglea (Figure 1C).

This staining pattern of SNARF-1 and SNARF-1 AM strongly suggested that we could successfully analyze the mesoglea on the basal side of the calciblastic epithelium, but to verify that we could image this layer we also stained microcolonies with the dye Col-F that binds to collagen (Biela et al., 2013), the main protein in the mesoglea (Gosline, 1971). Col-F fluorescence was strongest in the images obtained above the calciblastic cells on their basal side (Supplementary Material Figure S2), but absent from the calciblastic epithelium itself, consistent with the dye being cell impermeant (Biela et al., 2013) and confirming that we could accurately locate the mesoglea in our Z-stacks. Col-f also fluoresced strongly in sections of the collagen-rich mesoglea dissected from tentacles of the anemone of *A. viridis*, suggesting it was a reliable indicator of the mesoglea (Supplementary Material Figure S2).

Once satisfied we could visualize the mesoglea, we analyzed our SNARF-1 fluorescence ratios to determine pH in the ECM, calciblastic epithelium and mesoglea in light and darkness in seawater pH 8. Mean pH values are presented in Figure 1D and pH data were compared with a Kruskal Wallis test ($\chi^2(5,32) = 28.123$; $P < 0.001$) with *post hoc* analysis by Mann Whitney U pairwise comparisons. The mean mesoglea pH was pH 7.79 ± 0.15 (mean \pm SD) in the light, which was significantly higher than in the dark: 7.60 ± 0.08 . pH_{ECM} in the light was 8.28 ± 0.03 , significantly higher than in the dark 8.19 ± 0.04 . No light/dark differences were found in intracellular pH of the calcifying epithelium: pH 7.46 ± 0.04 (light) and 7.43 ± 0.02 (dark). Our measurements thus showed that mesoglea pH values were lower

than the corresponding pH_{ECM} values, lower than seawater pH and higher than pH_i in the calciblastic epithelium.

Effect of ocean acidification on the pH gradient across the calcifying epithelium

We determined pH in the mesoglea of coral microcolonies exposed to experimental ocean acidification for a 7-day period (Figure 2). These pH values are plotted with values of pH_{ECM} and pH_i of the calcifying epithelium obtained in the same corals and published previously in Venn et al., 2019 (Venn et al., 2019) (Figure 2A). Additionally, Figure 2A displays pH determined in the seawater surrounding the corals in the perfusion chamber during pH measurements. ECM, calcifying epithelium, and mesoglea pH data are also displayed as proton concentrations (Figure 2B). Together, this information provides us with a perspective of the proton gradient across the calcifying epithelium in light and darkness of coral microcolonies in conditions of acidification (Figure 2B).

Mesoglea pH decreased significantly in all acidification treatments (7.8, 7.4, 7.2) with respect to control seawater pH 8.0 (Two-way ANOVA; pH treatment $F_{3,25} = 39.932$, $P < 0.001$; light/dark $F_{1,25} = 2.917$, $P > 0.05$; interaction $F_{3,25} = 0.561$, $P > 0.05$; LSD *post hoc* analysis). There was no significant effect of light, and no significant interaction was observed between pH treatment and light/dark conditions. Decreases in pH_{ECM} followed the same pattern, with decreased pH_{ECM} in all acidification treatments with respect to seawater pH 8.0 (Two-way ANOVA; pH treatment $F_{3,25} = 163.531$, $P < 0.001$; light/dark $F_{1,25} = 0.037$, $P > 0.05$; interaction $F_{3,24} = 1.087$, $P > 0.05$ LSD *post hoc* analysis). Again, there was no significant effect of light, and no significant interaction was observed between pH treatment and light/dark conditions. Although both mesoglea pH and pH_{ECM} decreased significantly under acidification, the pH differences were greatest in the mesoglea. Decreases in mesoglea pH were 0.58 and 0.71 pH units in light and dark respectively between the seawater pH 8.0 and 7.2 treatments, but only decreased by 0.46 and 0.37 (light and dark) pH units in the ECM. The scale of these differences is clearer when displayed as $[H^+]$ in Figure 2B.

pH_i in the CE significantly decreased in the pH 7.4 and 7.2 treatments relative to the pH 8.0 treatment (Two-way ANOVA; pH treatment $F_{3,12} = 21.832$, $P < 0.001$; light/dark $F_{1,12} = 4.290$, $P > 0.05$; interaction $F_{3,12} = 0.255$, $P > 0.05$, LSD *post hoc* analysis). No significant effects of light/dark or an interaction were found. The significant decreases in pH_i of the calciblastic cells in the pH 7.4 and 7.2 treatments occur concomitantly with reversal of the proton gradient across the basal membrane as seawater pH decreases (Figure 2B). Specifically, at seawater pH 8.0, proton concentration was higher in the cells than the mesoglea, but at seawater pH 7.4 and below, this gradient switches with the basal mesoglea microenvironment

progressively becoming more acidic relative to the cells (higher $[H^+]$).

Effect of seawater [DIC] and TA on the pH gradient across the calcifying epithelium

To gain mechanistic insight into pH regulation by the calcifying cells, we determined pH on the basal side of the calciblastic epithelium in corals exposed to seawater in which pH was kept constant (~pH 7.9), but [DIC] was manipulated to higher or lower levels than ambient conditions (Figure 3). In Figure 3A, mesoglea pH values are plotted together with pH_{ECM} and calciblastic pH_i data that were obtained in the same corals and published previously in Comeau et al., 2017 (Comeau et al., 2017). Additionally, Figure 3A also displays pH determined in the seawater surrounding the corals in the perfusion chamber during pH measurements. Figure 3B illustrates the data as proton gradients across the calcifying cells in the different treatments.

Despite seawater pH remaining stable across the different treatments, mesoglea pH declined significantly in low and very low [DIC] treatments with respect to ambient and elevated [DIC] (Two-way ANOVA; [DIC] treatment $F_{3,21} = 57.356$, $P < 0.001$; light/dark $F_{1,21} = 11.783$, $P < 0.01$; interaction $F_{3,21} = 0.355$, $P > 0.05$ LSD *post hoc* analysis). Mesoglea pH was significantly higher in the light than dark, and no significant interaction was found between [DIC] treatment and light. Decreases in pH_{ECM} followed the same pattern, with decreased pH_{ECM} in low and very low [DIC] treatments with respect to ambient and elevated [DIC] (Two-way ANOVA; pH treatment $F_{3,25} = 53.900$, $P < 0.001$; light/dark $F_{1,25} = 18.889$, $P > 0.001$; interaction $F_{3,24} = 3.276$, $P > 0.05$ LSD *post hoc* analysis). pH_{ECM} was significantly higher in the light than dark, and a significant interaction was found between [DIC] treatment and light. In a similar fashion to what was observed in seawater acidification experiments, mesoglea pH changed to a much greater degree than pH_{ECM} in [DIC] experiments: a decline of approximately 0.9 pH units in the mesoglea between elevated and very low [DIC], versus a change of only 0.2–0.3 pH units in the pH_{ECM} in the same conditions.

In the calciblastic cells, pH_i decreased significantly in very low treatments relative to ambient and elevated [DIC] (Two-way ANOVA; pH treatment $F_{2,12} = 32.422$, $P < 0.001$; light/dark $F_{1,12} = 0.367$, $P > 0.05$; interaction $F_{2,12} = 0.302$, $P > 0.05$). However, these decreases were much smaller than the decreases in the mesoglea, causing reversal of the proton gradient across their basal membrane (Figure 3B). Calciblastic cell pH_i in the low [DIC] treatment is not given in Figure 3 as pH_i measurements were not made in this treatment (Comeau et al., 2017).

Discussion

pH regulation of the ECM by the calcifying cells promotes coral calcification because it elevates calcium carbonate saturation states and removes protons generated by the calcification process (McCulloch et al., 2012; Venn et al., 2013; Cyronak et al., 2016; Sevilgen et al., 2019; Sun et al., 2020). However, the cell physiology driving pH regulation of the calciblastic epithelium is not well understood. Here, we determined pH in the mesoglea to provide a transcellular perspective of the pH gradient across this cell layer. Measurements at ambient seawater of pH 8 (Figure 1) in light and darkness showed that pH in the mesoglea was lower than in the surrounding seawater and lower than pH_{ECM} on apical side of the calcifying epithelium (which was higher than the surrounding seawater). The existence of this pH gradient points to a mechanism of active pH regulation by the calciblastic epithelium that drives the net removal of acidity on its apical side (ECM) and net addition of acidity to the extracellular environment on its basal side (mesoglea). This indicates that the calciblastic epithelium is functionally polarized with respect to acid-base regulation with differential apical/basal localization of membrane bound transporters that act as ‘acid loaders’ and ‘acid extruders’ moving net acidity in and out of the cells (illustrated in Figure 4) (Spirli et al., 1998; Pickett et al., 2019). The terms ‘acid loaders’ and ‘acid extruders’ can apply to transporters encompassing those that transport either acid or base equivalents, such as H^+ and HCO_3^- (Boron, 2004). In cnidarians, functional polarity with respect to acid-base regulation has been previously described in the oral epithelia of anemones (Furla et al., 1998), but not in the coral calcifying cell layer. However, there are a number of examples of functionally polarized epithelia in other biomineralizing organisms including mammalian osteoblasts that load H^+ into the cells when removing protons produced by mineral deposition on bone collagen on their apical side and extrude H^+ on their basal membranes *via* Na^+/H^+ exchangers (NHE1) (Blair et al., 2018). In marine calcifiers, ionocytes in the inner ear of teleost fish remove H^+ and add HCO_3^- to the endolymph fluid generating a gradient of 0.5 pH units between the site of otolith growth and the blood (Kwan et al., 2020; Kwan and Tresguerres, 2022).

Previous studies of ion transporters in *S. pistillata* have identified candidate proteins by immunolocalization and differential gene expression that could perform the acid loader and acid extruder roles underlying functional polarity of the calciblastic epithelium. Candidate acid loaders on the apical membrane of the calcifying epithelium (driving increases in pH_{ECM}) could include Ca^{2+} ATPases that exchange H^+ for Ca^{2+} (Zoccola et al., 2004), HCO_3^-/Cl^- exchangers (SLC4γ) (Zoccola et al., 2015) and ammonium transporters (AMT) (Capasso et al., 2021) that have been localized to the calcifying epithelium in *S.*

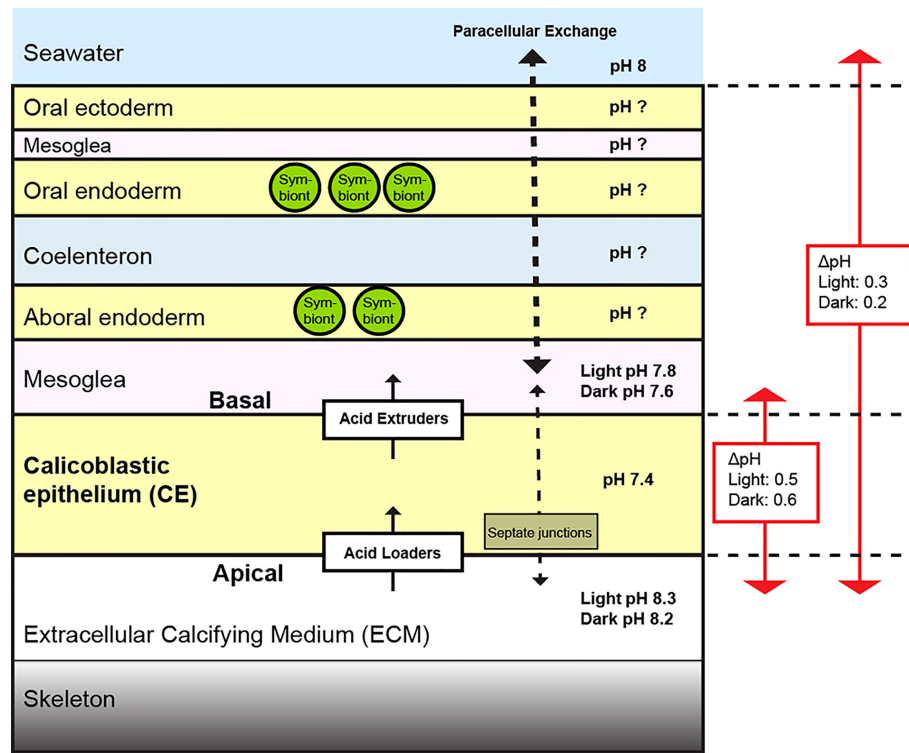


FIGURE 4

Diagram depicting proposed factors involved in pH regulation of the ECM by the calcicoblastic epithelium (CE) at the growing edge of *S. pistillata* in seawater pH 8. Regulation of pH on the apical side of the CE occurs via net acid loaders. On the basal membrane of the CE there are acid extruders that decrease pH in the mesoglea. Paracellular permeability is greater between seawater and the mesoglea (thicker dashed arrow) than between the mesoglea and the ECM due to properties of septate junctions in the CE (Tambutté et al., 2011). The pH gradient between the ECM and mesoglea is different to that between the ECM and seawater. The pH gradients between the ECM and other tissue layers are currently not known and an important area of future research.

pistillata with immunohistochemistry. On the basal side of the calcifying epithelium, candidate acid extruders that drive decreases in mesoglea pH could include a voltage gated proton channel (spiHvCN1.1) shown to be more highly expressed in aboral tissue (Capasso et al., 2021), ubiquitously expressed bicarbonate transporters belonging to the SLC26 and SLC4 families, Na/H⁺ exchangers (SLC9A1) and Vacuolar-type electrogenic H⁺-ATP hydrolases (Capasso et al., 2021). Previous work on *S. pistillata* has also identified cytosolic and secreted or membrane bound carbonic anhydrases, that catalyze pH dependent interconversion of CO₂ and HCO₃⁻, which are likely to be involved in calcicoblastic epithelium pH regulation (Bertucci et al., 2013). More work is required to understand the role of all these proteins in corals and to investigate other candidates including otopetrin proton channels that have recently been shown to be critical for biomineralization in other marine calcifiers (Chang et al., 2021).

In addition to identifying membrane transporters with possible apical and basal roles in pH regulation of the calcicoblastic epithelium, previous research on *S. pistillata* has also shown that corals possess intercellular junctions that may

regulate the passive diffusion of ions and molecules across the epithelium by paracellular transport (Tambutté et al., 2012; Ganot et al., 2014). Molecular studies have shown that corals possess septate junctions, the invertebrate counterpart of vertebrate tight junctions (Ganot et al., 2014), and complementary electrophysiological studies suggest that these junctions exert control over the degree of passive ion flux via the paracellular pathway (Tambutté et al., 2012; Taubner et al., 2017). Junctions are widely known to play a prominent role in establishing functional polarity and maintaining transepithelial ion/pH gradients in other organisms (Shen, 2012; Pickett et al., 2019), and their presence is likely to contribute to the pH gradient across the calcicoblastic epithelium.

Light

Previous research has shown that light is an important environmental factor influencing both photosymbiotic coral pH regulation (Venn et al., 2009; Venn et al., 2011; Venn et al., 2019) and calcification (Gattuso et al., 1999; Moya, 2006;

Cohen et al., 2016). Our measurements of pH in the mesoglea at seawater pH 8 (Figure 1) showed how irradiance leads to an increase in mesoglea pH with respect to darkness and that this was accompanied by a significant but smaller increase in pH in the ECM. In contrast, pH_i in the calcifying epithelium remained stable in light and darkness, consistent with previous observations of calciblastic epithelium pH_i (Venn et al., 2011).

The observed light-dark shifts in pH of the ECM and mesoglea presumably occur due to photosynthetic activity of the symbionts in the overlying endoderm layers. This is consistent with the numerous previous studies proposing that symbiont photosynthesis provides a favorable gradient for the transport of protons produced by calcification away from the ECM (Goreau, 1959; Gattuso et al., 1999; Furla et al., 2000; Allemand et al., 2004; Jokiel P. L., 2011; Comeau et al., 2013). While the exact mechanism of how symbiont photosynthesis enhances removal of protons from the ECM is not clear, our observations of light induced elevations in mesoglea pH indicate that light could create a favorable gradient for acid extrusion on the basal side of the calcifying epithelium. Importantly, this may facilitate acid loading on the apical side of the calcifying epithelium which results in the observed increases in pH in the ECM. Stable calciblastic epithelium pH_i suggests that the balance of activity in the acid loaders and acid extruders is maintained in these conditions (Leem et al., 1999; Boron, 2004). These ideas require further investigation.

Significant light-driven increases of both mesoglea pH and pH_{ECM} were also observed in the seawater [DIC] experiments, however in seawater acidification experiments neither variable changed significantly. The lack of a significant response to light in the seawater acidification experiment cannot easily be explained, but it could be linked to the fact that the growing edge of laterally growing colonies (where pH analysis was carried out) is an area with low symbiont density (Jokiel P. L., 2011; Venn et al., 2011). As such, if colonies in the seawater acidification experiment had lower symbiont densities at the growing edge compared to those in the seawater [DIC] experiments then the influence of photosynthesis on pH in the mesoglea and ECM could have been weaker. Future work could investigate this possibility by investigating pH gradients in symbiont-dense regions of coral colonies and areas of low symbiont density including the rapidly calcifying branch tips. This will be technically challenging and will require the development of new techniques, as currently the growing edge is the only area where the calcifying epithelium can be analyzed *in vivo*.

Despite the discrepancies in the effect of light between the experiments, the relationship between mesoglea pH and pH_{ECM} was consistent (i.e. if light causes mesoglea pH to increase then so does pH_{ECM}). Indeed, pooled mean values of pH in the mesoglea from all three experiments in light and darkness were significantly correlated with the corresponding mean values of pH_{ECM} (Supplementary Figure S3).

Ocean acidification

The effect of seawater acidification on pH_i and pH_{ECM} has been characterized previously (Venn et al., 2019), and the current study revealed how pH in the mesoglea responded in the same conditions. Putting these data together in Figure 2 provides functional insight into how the calcifying epithelium behaves under acidification.

The first important observation was that pH in the mesoglea was not only more acidic than the ECM and seawater, but also decreased to a much greater extent than the ECM in the seawater acidification treatments. This is especially evident in Figure 2B when viewed as $[H^+]$. These data indicate that the ECM is relatively well regulated with respect to pH, but the mesoglea is more pH conforming with respect to the external seawater environment. The basis of this differential regulation may lie not only in differences in the behavior of membrane transporters implicated in pH regulation, but also in differences in paracellular transport across the tissues that separate the mesoglea and ECM from seawater. Previous electrophysiological work carried out on coral tissue paracellular permeability suggests that the septate junctions exert tighter control over paracellular permeability in the calciblastic epithelium than the overlying tissue layers such the endoderm layers (Bénazet-Tambutté et al., 1996; Tambutté et al., 2012). Based on these studies and our data, we suggest that the mesoglea is relatively open to paracellular exchange *via* the overlying aboral endoderm and is therefore influenced by pH of the overlying coelenteron and surrounding seawater. By contrast, the ECM may be better regulated with respect to pH due to the tighter characteristics of the septate junctions in the calcifying epithelium that restrict paracellular exchange with the overlying layers and seawater (illustrated in Figure 4). In the context of seawater acidification, it should be noted that previous research on *S. pistillata* indicates that paracellular permeability is increased (loosened) by seawater acidification, possibly by the effect of low pH on septate junction protein conformation and interaction (Venn et al., 2020). This loosening effect would presumably increase the challenge of regulating pH in the ECM because the paracellular flux of protons between the mesoglea and the ECM could increase. The permeability of coral septate junctions is thought to be ion-selective (Taubner et al., 2017), but more research on the permeability of the calcifying epithelium is required to test these ideas.

Another important observation from the seawater acidification experiments was that mesoglea pH remains below seawater pH in all conditions of acidification. This suggests that there is a combined effect of proton extrusion on the basal side of the calciblastic epithelium and their accumulation in the mesoglea due to a less favorable gradient for their flux to the external seawater (Jokiel P., 2011). At seawater pH 7.4 and below, mesoglea pH declined to a point in which its values were actually lower than the pH_i of the calcifying epithelium, leading to a reversal of the proton gradient across the basal membrane.

Interestingly, significant decreases in pH_i of the CE also occur in the seawater pH 7.4 and pH 7.2 treatments, suggesting that the reversal in the proton gradient is a physiological tipping point for the calciblastic cells to maintain acid-base homeostasis at their normal pH_i of 7.4. This may occur if the equilibrium potential of H^+ across the basal membrane is disrupted by the reversal of the pH gradient with possible consequences on membrane potential and the function of transporters with both acid loading and acid extrusion roles (Madshus, 1988; Bondarenko, 1997; Leem et al., 1999; Boron, 2004; Casey et al., 2010; Hulikova et al., 2011). Significant decreases in pH_i are anticipated to be detrimental to the cells generally, as virtually all intracellular processes are pH-sensitive, and pH_i is normally tightly regulated (Madshus, 1988; Casey et al., 2010).

Variation of seawater [DIC] and TA

Our previous study, Comeau et al., 2017 (Comeau et al., 2017), reported that decreases in seawater [DIC] lead to declines in the pH_{ECM} and CE calciblastic epithelium pH_i even under constant seawater pH. The current study builds on this work by revealing that these declines are associated with a large drop in pH in the mesoglea, causing a pronounced change in the transepithelial pH gradient across the calcifying epithelium. The mechanism explaining the declines in pH in the mesoglea in low and very low [DIC] treatments maybe related to the lower total alkalinity (TA) (i.e. buffering capacity) of seawater in this treatments. Assuming paracellular exchange between seawater and the mesoglea (discussed above), then low and very low [DIC] treatments may result in a lower buffering capacity of the mesoglea. Acid extrusion mechanisms (either proton extrusion or HCO_3^- uptake) on the basal side of the calcifying epithelium would then acidify the mesoglea to greater levels than in ambient and elevated [DIC] treatments. The resulting lower pH in the mesoglea could lead to an acid-base regulatory challenge to the CE leading to the observed decreases in pH_i and pH_{ECM} .

Further investigations are required to better understand our findings, but when considering the seawater acidification and [DIC] experiment together, the results point to a combined role of protons and HCO_3^- in influencing the pH across the CE. This fits with what is known about classical pH regulation in vertebrate and invertebrate epithelia that involve movement of both HCO_3^- and protons (Boron, 2004). A dual role of H^+ and HCO_3^- is also consistent with the observation of Comeau et al. (2017) that [DIC]/ $[\text{H}^+]$, $[\text{CO}_3^{2-}]$ and TA all correlate with pH_{ECM} level (expressed as $[\text{H}^+]$). Together these results strongly suggest that balance in the concentration of H^+ and DIC strongly shape the transepithelial pH gradients across the calcifying epithelium. These observations also complement analyses by others (Jokiel P., 2011; Cyronak et al., 2016) who described how the seawater [DIC]/ $[\text{H}^+]$ ratio and $[\text{CO}_3^{2-}]$ also correlates with coral calcification rates.

Conclusions and perspectives

There are three important conclusions to our study. Firstly, the pH gradient across the calcifying epithelium indicates that it is functionally polarized with respect to acid-base regulation. Active transcellular transport by acid loaders and acid extruders, and regulation of paracellular transport are likely factors contributing to this functional polarity. Functional studies are needed to investigate whether candidate transporters that have been localized to the calcifying epithelium in previous studies e.g. (Zoccola et al., 2004; Zoccola et al., 2015) have a role in driving the pH gradients observed here.

Secondly, we observed that pH in the microenvironment on the basal side of the calcifying cell layer is distinct to the surrounding seawater. As such, the pH offset between the ECM and the mesoglea is different to the offset between the ECM and seawater (Figure 4). This has implications when we build numerical and conceptual models of the coral calcification mechanism at the cellular or organism level (Edmunds et al., 2016), particularly ion exchange between the environment, mesoglea and ECM and the energetics of pH regulation for calcification (Ries, 2011; Gagnon et al., 2012; Hohn and Merico, 2012; Nakamura et al., 2013; Venn et al., 2013; Guo, 2019; Gagnon et al., 2021). Furthermore, the field of coral calcification is rapidly evolving, and future models will also need to take into account that the first steps of calcification involve production of amorphous calcium carbonate (ACC) in the calciblastic cells which is released into the ECM where ion by ion growth of crystals occurs (Mass et al., 2017; Schmidt et al., 2022). The findings of the current study are relevant when considering both protons generated during production of ACC within calciblastic cells and protons loaded at the apical side from the ECM, since in both cases these protons need to be extruded from calciblastic cells. The current study suggests that this would occur *via* acid extrusion on the basal membrane of the calcifying epithelium.

Thirdly, environmental factors impact the pH gradient across the calcifying epithelium, which ultimately effects pH_{ECM} . Irradiance increases pH_{ECM} and pH in the mesoglea in parallel, suggesting that photosynthesis ameliorates proton transport across the calcifying epithelium by providing a more favorable gradient for acid extrusion on its basal side. Experimental ocean acidification and manipulation of seawater [DIC] and TA revealed that pH is more variable in the mesoglea than the ECM, suggesting that the mesoglea is relatively open to the influence of external changes in pH and carbonate chemistry, whereas the ECM is tightly regulated. We therefore suggest that environmental effects on pH_{ECM} , such as ocean acidification, modulates pH_{ECM} by steepening the proton gradients across the calciblastic epithelium and increasing the acid-base regulatory challenge.

Looking forward, future research needs to look at pH gradients deeper within the coral tissues because currently the exact pH

gradients between the other tissues layers and extracellular compartments are unknown (Figure 4). Although there have been measurements of pH made in the coelenteron of other coral species (Kühl et al., 1995; Al-Horani et al., 2003; Bove et al., 2020), accurate characterization of pH gradients across the tissues will rely on working in a single model species under controlled conditions, because absolute pH values in the various layers are likely to vary between species and environmental conditions.

Although the current study and future research proposed here are essentially lab based, this type of mechanistic physiological research in corals is becoming increasingly important (Weis et al., 2008; Weis, 2019). Coral reef restoration research is exploring methods for identifying and cultivating stress-resistant corals that include innovative but challenging approaches such as gene-editing and selective breeding (van Oppen et al., 2015; Anthony et al., 2017). Harnessing traits related to coral stress resistance, such as pH regulation against acidification, ultimately relies on deepening our understanding of the underlying physiological mechanisms.

Data availability statement

The datasets presented in this study can be found in online repositories. The names of the repository/repositories and accession number(s) can be found below: Pangaea online database (Data submission 2022-06-07T12:21:02Z) under processing.

Author contributions

AV, ET, SC, and ST carried out research, contributed to the conception and design of the study and analyzed data. AV and ST wrote the manuscript. All authors contributed to the article and approved the submitted version.

References

- Adkins, J. F., Boyle, E. A., Curry, W. B., and Lutringer, A. (2003). Stable isotopes in deep-sea corals and a new mechanism for “vital effects.” *Geochim. Cosmochim. Acta* 67, 1129–1143. doi: 10.1016/S0016-7037(02)01203-6
- Al-Horani, F. A., Al-Moghrabi, S. M., and de Beer, D. (2003). The mechanism of calcification and its relation to photosynthesis and respiration in the scleractinian coral *Galaxea fascicularis*. *Mar. Biol.* 142, 419–426. doi: 10.1007/s00227-002-0981-8
- Allemand, D., Ferrier-Pagès, C., Furla, P., Houlbrèque, F., Puverel, S., Reynaud, S., et al. (2004). Biomineralisation in reef-building corals: from molecular mechanisms to environmental control. *Comptes Rendus Palevol* 3, 453–467. doi: 10.1016/j.crpv.2004.07.011
- Anthony, K., Bay, L. K., Costanza, R., Firn, J., Gunn, J., Harrison, P., et al. (2017). New interventions are needed to save coral reefs. *Nat. Ecol. Evol.* 1, 1420–1422. doi: 10.1038/s41559-017-0313-5
- Bénazet-Tambutté, S., Allemand, D., and Jaubert, J. (1996). Permeability of the oral epithelial layers in cnidarians. *Mar. Biol.* 126, 43–53. doi: 10.1007/BF00571376
- Bertucci, A., Moya, A., Tambutté, S., Allemand, D., Supuran, C. T., and Zoccola, D. (2013). Carbonic anhydrases in anthozoan corals—a review. *Bioorg. Med. Chem.* 21, 1437–1450. doi: 10.1016/j.bmc.2012.10.024
- Biela, E., Galas, J., Lee, B., Johnson, G. L., Darzynkiewicz, Z., and Dobrucki, J. W. (2013). Col-f, a fluorescent probe for ex vivo confocal imaging of collagen and elastin in animal tissues. *Cytometry A* 83, 533–539. doi: 10.1002/cyto.a.22264
- Blair, H. C., Larrouture, Q. C., Tourkova, I. L., Liu, L., Bian, J. H., Stolz, D. B., et al. (2018). Support of bone mineral deposition by regulation of pH. *Am. J. Physiol. Cell Physiol.* 315, C587–C597. doi: 10.1152/ajpcell.00056.2018
- Bondarenko, A. I. (1997). Effect of acidosis on the membrane potential of intact guinea pig aortic endothelial cells. *Neurophysiology* 29, 104–107. doi: 10.1007/BF02463223
- Boron, W. F. (2004). Regulation of intracellular pH. *Adv. Physiol. Educ.* 28, 160–179. doi: 10.1152/advan.00045.2004
- Bove, C., Whitehead, R., and Szmant, A. (2020). Responses of coral gastrovascular cavity pH during light and dark incubations to reduced seawater pH suggest species-specific responses to the effects of ocean acidification on calcification. *Coral Reefs* 39:1675–1691. doi: 10.1007/s00338-020-01995-7
- Capasso, L., Ganot, P., Planas-Bielsa, V., Tambutté, S., and Zoccola, D. (2021). Intracellular pH regulation: characterization and functional investigation of h+

Funding

This research was funded by the Government of the Principality of Monaco.

Acknowledgments

We thank Natacha Segonds, Nathalie Techer, Dominique Desgré and Eric Elia for technical assistance and coral culture.

Conflict of interest

The authors declare that the research was conducted in the absence of any commercial or financial relationships that could be construed as a potential conflict of interest.

Publisher's note

All claims expressed in this article are solely those of the authors and do not necessarily represent those of their affiliated organizations, or those of the publisher, the editors and the reviewers. Any product that may be evaluated in this article, or claim that may be made by its manufacturer, is not guaranteed or endorsed by the publisher.

Supplementary material

The Supplementary Material for this article can be found online at: <https://www.frontiersin.org/articles/10.3389/fmars.2022.973908/full#supplementary-material>

- transporters in stylophora pistillata. *BMC Mol. Cell Biol.* 22, 18. doi: 10.1186/s12860-021-00353-x
- Casey, J. R., Grinstein, S., and Orlowski, J. (2010). Sensors and regulators of intracellular pH. *Nat. Rev. Mol. Cell Biol.* 11, 50–61. doi: 10.1038/nrm2820
- Chang, W., Matt, A.-S., Schewe, M., Musinszki, M., Grüssel, S., Brandenburg, J., et al. (2021). An otopetrin family proton channel promotes cellular acid efflux critical for biomineralization in a marine calcifier. *Proc. Natl. Acad. Sci. U. S. A.* 118 (30). doi: 10.1073/pnas.2101378118
- Cohen, I., Dubinsky, Z., and Erez, J. (2016). Light enhanced calcification in hermatypic corals: New insights from light spectral responses. *Front. Mar. Sci.* 2. doi: 10.3389/fmars.2015.00122
- Comeau, S., Carpenter, R. C., and Edmunds, P. J. (2013). Coral reef calcifiers buffer their response to ocean acidification using both bicarbonate and carbonate. *Proc. R. Soc. B Biol. Sci.* 280, 20122374. doi: 10.1098/rspb.2012.2374
- Comeau, S., Cornwall, C. E., DeCarlo, T. M., Doo, S. S., Carpenter, R. C., and McCulloch, M. T. (2019). Resistance to ocean acidification in coral reef taxa is not gained by acclimatization. *Nat. Clim. Change* 9, 477–483. doi: 10.1038/s41558-019-0486-9
- Comeau, S., Cornwall, C. E., Shlesinger, T., Hoogenboom, M., Mana, R., McCulloch, M. T., et al. (2022). pH variability at volcanic CO₂ seeps regulates coral calcifying fluid chemistry. *Glob. Change Biol.* 28, 2751–2763. doi: 10.1111/gcb.16093
- Comeau, S., Tambutté, E., Carpenter, R. C., Edmunds, P. J., Evensen, N. R., Allemand, D., et al. (2017). Coral calcifying fluid pH is modulated by seawater carbonate chemistry not solely seawater pH. *Proc. Biol. Sci.* 284:20161669. doi: 10.1098/rspb.2016.1669
- Cyronak, T., Schulz, K. G., and Jokiel, P. L. (2016). The omega myth: what really drives lower calcification rates in an acidifying ocean. *ICES J. Mar. Sci.* 73, 558–562. doi: 10.1093/icesjms/fsv075
- Drake, J. L., Mass, T., Stolarski, J., Von Euw, S., van de Schootbrugge, B., and Falkowski, P. G. (2020). How corals made rocks through the ages. *Glob. Change Biol.* 26, 31–53. doi: 10.1111/gcb.14912
- Edmunds, P. J., Comeau, S., Lantz, C., Andersson, A., Briggs, C., Cohen, A., et al. (2016). Integrating the effects of ocean acidification across functional scales on tropical coral reefs. *Bioscience* 66, 350–362. doi: 10.1093/biosci/biw023
- Fietzke, J., and Wall, M. (2022). Distinct fine-scale variations in calcification control revealed by high-resolution 2D boron laser images in the cold-water coral *Lophelia pertusa*. *Sci. Adv.* 8, eabj4172. doi: 10.1126/sciadv.abj4172
- Furla, P., Bénazet-Tambutté, S., Jaubert, J., and Allemand, D. (1998). Functional polarity of the tentacle of the sea anemone *Anemonia viridis*: role in inorganic carbon acquisition. *Am. J. Physiol. Integr. Comp. Physiol.* 274, R303–R310. doi: 10.1152/ajpregu.1998.274.2.R303
- Furla, P., Galgani, I., Durand, I., and Allemand, D. (2000). Carbon sources for coral calcification and photosynthesis. *J. Exp. Biol.* 203, 3445–3457. doi: 10.1242/jeb.203.22.3445
- Gagnon, A. C., Adkins, J. F., and Erez, J. (2012). Seawater transport during coral biomineralization. *Earth Planet. Sci. Lett.* 329–330, 150–161. doi: 10.1016/j.epsl.2012.03.005
- Gagnon, A. C., Gothmann, A. M., Branson, O., Rae, J. W. B., and Stewart, J. A. (2021). Controls on boron isotopes in a cold-water coral and the cost of resilience to ocean acidification. *Earth Planet. Sci. Lett.* 554, 116662. doi: 10.1016/j.epsl.2020.116662
- Ganot, P., Zoccola, D., Tambutté, E., Voolstra, C. R., Aranda, M., Allemand, D., et al. (2014). Structural molecular components of septate junctions in cnidarians point to the origin of epithelial junctions in eukaryotes. *Mol. Biol. Evol.* 32, 44–62. doi: 10.1093/molbev/msu265
- Gattuso, J., Allemand, D., and Frankignoulle, M. (1999). Photosynthesis and calcification at cellular, organismal and community levels in coral reefs: A review on interactions and control by carbonate chemistry. *Am. Zool.* 39, 160–183. doi: 10.1093/icb/39.1.160
- Gilbert, P. U. P. A., Bergmann, K. D., Boekelheide, N., Tambutté, S., Mass, T., Marin, F., et al. (2022). Biomineralization: Integrating mechanism and evolutionary history. *Sci. Adv.* 8, eabl9653. doi: 10.1126/sciadv.abl9653
- Goreau, T. (1959). The physiology of skeleton formation in corals. i. a method for measuring the rate of calcium deposition by corals under different conditions. *Biol. Bull.*, 116 (1), 59–75. doi: 10.2307/1539156
- Gosline, J. M. (1971). Connective tissue mechanics of metridium senile: I. structural and compositional aspects. *J. Exp. Biol.* 55, 763–774. doi: 10.1242/jeb.55.3.763
- Guo, W. (2019). Seawater temperature and buffering capacity modulate coral calcifying pH. *Sci. Rep.* 9, 1189. doi: 10.1038/s41598-018-36817-y
- Hohn, S., and Merico, A. (2012). Modelling coral polyp calcification in relation to ocean acidification. *Biogeosciences* 9, 4441–4454. doi: 10.5194/bg-9-4441-2012
- Hulikova, A., Vaughan-Jones, R., and Swietach, P. (2011). Dual role of CO₂/HCO₃ buffer in the regulation of intracellular pH of three-dimensional tumor growths. *J. Biol. Chem.* 286, 13815–13826. doi: 10.1074/jbc.M111.219899
- Jokiel, P. (2011). Ocean acidification and control of reef coral calcification by boundary layer limitation of proton flux. *Bull. Mar. Sci.* 87, 639–657. doi: 10.5343/bms.2010.1107
- Jokiel, P. L. (2011). The reef coral two compartment proton flux model: A new approach relating tissue-level physiological processes to gross coralium morphology. *J. Exp. Mar. Bio. Ecol.* 409, 1–12. doi: 10.1016/j.jembe.2011.10.008
- Kühl, M., Cohen, Y., Dalsgaard, T., Jørgensen, B., and Revsbech, N. (1995). Microenvironment and photosynthesis of zooxanthellae in scleractinian corals studied with microsensors for O₂, pH and light. *Marine Ecology Progress Series* 117, 159–177. doi: 10.3354/meps117159
- Kwan, G. T., Smith, T. R., and Tresguerres, M. (2020). Immunological characterization of two types of ionocytes in the inner ear epithelium of pacific chub mackerel (*Scomber japonicus*). *J. Comp. Physiol. B* 190, 419–431. doi: 10.1007/s00360-020-01276-3
- Kwan, G. T., and Tresguerres, M. (2022). Elucidating the acid-base mechanisms underlying otolith overgrowth in fish exposed to ocean acidification. *Sci. Total Environ.* 823, 153690. doi: 10.1016/j.scitotenv.2022.153690
- Leem, C. H., Lagadic-Gossmann, D., and Vaughan-Jones, R. D. (1999). Characterization of intracellular pH regulation in the guinea-pig ventricular myocyte. *J. Physiol.* 517, 159–180. doi: 10.1111/j.1469-7793.1999.0159z.x
- Madhus, I. H. (1988). Regulation of intracellular pH in eukaryotic cells. *Biochem. J.* 250, 1–8. doi: 10.1042/bj2500001
- Mass, T., Giuffrè, A. J., Sun, C.-Y., Stifler, C. A., Frazier, M. J., Neder, M., et al. (2017). Amorphous calcium carbonate particles form coral skeletons. *Proc. Natl. Acad. Sci.* 114, E7670–E7678. doi: 10.1073/pnas.1707901114
- McCulloch, M. T., D'Olivo, J. P., Falter, J., Holcomb, M., and Trotter, J. A. (2017). Coral calcification in a changing world and the interactive dynamics of pH and DIC upregulation. *Nat. Commun.* 8, 15686. doi: 10.1038/ncomms15686
- McCulloch, M., Falter, J., Trotter, J., and Montagna, P. (2012). Coral resilience to ocean acidification and global warming through pH up-regulation. *Nat. Clim. Change* 2, 623–627. doi: 10.1038/nclimate1473
- Moya, A. (2006). Study of calcification during a daily cycle of the coral *Stylophora pistillata*: implications for 'light-enhanced calcification'. *J. Exp. Biol.* 209, 3413–3419. doi: 10.1242/jeb.02382
- Muscantine, L., Tambutté, E., and Allemand, D. (1997). Morphology of coral desmocytes, cells that anchor the calciblastic epithelium to the skeleton. *Coral Reefs* 16, 205–213. doi: 10.1007/s003380050075
- Nakamura, T., Nadaoka, K., and Watanabe, A. (2013). A coral polyp model of photosynthesis, respiration and calcification incorporating a transcellular ion transport mechanism. *Coral Reefs* 32, 779–794. doi: 10.1007/s00338-013-1032-2
- Neder, M., Laissue, P. P., Akiva, A., Akkaynak, D., Albéric, M., Spaeker, O., et al. (2019). Mineral formation in the primary polyps of pocilloporoid corals. *Acta Biomater.* 96, 631–645. doi: 10.1016/j.actbio.2019.07.016
- Ohno, Y., Iguchi, A., Shinzato, C., Gushi, M., Inoue, M., Suzuki, A., et al. (2017a). Calcification process dynamics in coral primary polyps as observed using a calcein incubation method. *Biochem. Biophys. Rep.* 9, 289–294. doi: 10.1016/j.bbrep.2017.01.006
- Ohno, Y., Iguchi, A., Shinzato, C., Inoue, M., Suzuki, A., Sakai, K., et al. (2017b). An aposymbiotic primary coral polyp counteracts acidification by active pH regulation. *Sci. Rep.* 7, 40324. doi: 10.1038/srep40324
- Parisi, M. G., Grimaldi, A., Baranzini, N., La Corte, C., Dara, M., Parrinello, D., et al. (2021). Mesoglea extracellular matrix reorganization during regenerative process in *Anemonia viridis* (Forsk.) (Forsk.) (1775). *Int. J. Mol. Sci.* 22, 5971. doi: 10.3390/ijms22115971
- Pickett, M. A., Naturale, V. F., and Feldman, J. L. (2019). A polarizing issue: Diversity in the mechanisms underlying apico-basolateral polarization. *In vivo. Annu. Rev. Cell Dev. Biol.* 35, 285–308. doi: 10.1146/annurev-cellbio-100818-125134
- Raz-Bahat, M., Erez, J., and Rinkevich, B. (2006). *In vivo* light-microscopic documentation for primary calcification processes in the hermatypic coral *Stylophora pistillata*. *Cell Tissue Res.* 325, 361–368. doi: 10.1007/s00441-006-0182-8
- Ries, J. B. (2011). A physicochemical framework for interpreting the biological calcification response to CO₂-induced ocean acidification. *Geochim. Cosmochim. Acta* 75, 4053–4064. doi: 10.1016/j.gca.2011.04.025
- Schmidt, C. A., Stifler, C. A., Luffey, E. L., Fordyce, B. I., Ahmed, A., Barreiro Pujol, G., et al. (2022). Faster crystallization during coral skeleton formation correlates with resilience to ocean acidification. *J. Am. Chem. Soc.* 144, 1332–1341. doi: 10.1021/jacs.1c11434
- Sevilgen, D. S., Venn, A. A., Hu, M. Y., Tambutté, E., de Beer, D., Planas-Bielsa, V., et al. (2019). Full *in vivo* characterization of carbonate chemistry at the site of calcification in corals. *Sci. Adv.* 5, eaau7447. doi: 10.1126/sciadv.aau7447

- Shen, L. (2012). Tight junctions on the move: molecular mechanisms for epithelial barrier regulation. *Ann. N. Y. Acad. Sci.* 1258, 9–18. doi: 10.1111/j.1749-6632.2012.06613.x
- Sheppard, C., Davy, S., Pilling, G., and Graham, N. (2017). *The biology of coral reefs. 2nd ed* (Oxford: Oxford University Press). doi: 10.1093/oso/9780198787341.001.0001
- Sinclair, D. J., and Risk, M. J. (2006). A numerical model of trace-element coprecipitation in a physicochemical calcification system: Application to coral biomineralization and trace-element 'vital effects'. *Geochim. Cosmochim. Acta* 70, 3855–3868. doi: 10.1016/j.gca.2006.05.019
- Spirli, C., Granato, A., Zsembery, A., Anglani, F., Okolicsányi, L., LaRusso, N. F., et al. (1998). Functional polarity of Na⁺/H⁺ and Cl⁻/HCO₃⁻ exchangers in a rat cholangiocyte cell line. *Am. J. Physiol. Liver Physiol.* 275, G1236–G1245. doi: 10.1152/ajpgi.1998.275.6.G1236
- Sun, C.-Y., Stifler, C. A., Chopdekar, R. V., Schmidt, C. A., Parida, G., Schoeppler, V., et al. (2020). From particle attachment to space-filling coral skeletons. *Proc. Natl. Acad. Sci.* 117, 30159 LP–30170. doi: 10.1073/pnas.2012025117
- Tambutté, S., Holcomb, M., Ferrier-Pagès, C., Reynaud, S., Tambutté, É., Zoccola, D., et al. (2011). Coral biomineralization: From the gene to the environment. *J. Exp. Mar. Bio. Ecol.* 408, 58–78. doi: 10.1016/j.jembe.2011.07.026
- Tambutté, E., Tambutté, S., Segonds, N., Zoccola, D., Venn, A., Erez, J., et al. (2012). Calcein labelling and electrophysiology: insights on coral tissue permeability and calcification. *Proc. R. Soc B Biol. Sci.* 279, 19–27. doi: 10.1098/rspb.2011.0733
- Taubner, I., Böhm, F., Eisenhauer, A., Tambutté, E., Tambutté, S., Moldzio, S., et al. (2017). An improved approach investigating epithelial ion transport in scleractinian corals. *Limnol. Oceanogr. Methods* 15, 753–765. doi: 10.1002/lom3.10194
- van Oppen, M. J. H., Oliver, J. K., Putnam, H. M., and Gates, R. D. (2015). Building coral reef resilience through assisted evolution. *Proc. Natl. Acad. Sci.* 112, 2307–2313. doi: 10.1073/pnas.1422301112
- Venn, A. A., Bernardet, C., Chabenat, A., Tambutté, E., and Tambutté, S. (2020). Paracellular transport to the coral calcifying medium: effects of environmental parameters. *J. Exp. Biol.* 223, jeb227074. doi: 10.1242/jeb.227074
- Venn, A. A., Tambutté, E., Caminiti-Segonds, N., Techer, N., Allemand, D., and Tambutté, S. (2019). Effects of light and darkness on pH regulation in three coral species exposed to seawater acidification. *Sci. Rep.* 9, 2201. doi: 10.1038/s41598-018-38168-0
- Venn, A. A., Tambutté, E., Holcomb, M., Allemand, D., and Tambutté, S. (2011). Live tissue imaging shows reef corals elevate pH under their calcifying tissue relative to seawater. *PLoS One.* 6(5): e20013. doi: 10.1371/journal.pone.0020013
- Venn, A. A., Tambutté, E., Holcomb, M., Laurent, J., Allemand, D., and Tambutté, S. (2013). Impact of seawater acidification on pH at the tissue-skeleton interface and calcification in reef corals. *Proc. Natl. Acad. Sci.* 110, 1634 LP–1639. doi: 10.1073/pnas.1216153110
- Venn, A. A., Tambutté, E., Lotto, S., Zoccola, D., Allemand, D., and Tambutté, S. (2009). Imaging intracellular pH in a reef coral and symbiotic anemone. *Proc. Natl. Acad. Sci. U. S. A.* 106, 16574–16579. doi: 10.1073/pnas.0902894106
- Wall, M., Fietzke, J., Schmidt, G. M., Fink, A., Hofmann, L. C., de Beer, D., et al. (2016). Internal pH regulation facilitates *in situ* long-term acclimation of massive corals to end-of-century carbon dioxide conditions. *Sci. Rep.* 6, 30688. doi: 10.1038/srep30688
- Weis, V. M. (2019). Cell biology of coral symbiosis: Foundational study can inform solutions to the coral reef crisis. *Integr. Comp. Biol.* 59, 845–855. doi: 10.1093/icb/icz067
- Weis, V. M., Davy, S. K., Hoegh-Guldberg, O., Rodriguez-Lanetty, M., and Pringle, J. R. (2008). Cell biology in model systems as the key to understanding corals. *Trends Ecol. Evol.* 23(7), 369–376. doi: 10.1016/j.tree.2008.03.004
- Zoccola, D., Ganot, P., Bertucci, A., Caminiti-Segonds, N., Techer, N., Voolstra, C. R., et al. (2015). Bicarbonate transporters in corals point towards a key step in the evolution of cnidarian calcification. *Sci. Rep.* 5, 9983. doi: 10.1038/srep09983
- Zoccola, D., Tambutté, E., Kulhanek, E., Puverel, S., Scimeca, J. C., Allemand, D., et al. (2004). Molecular cloning and localization of a PMCA p-type calcium ATPase from the coral *Stylophora pistillata*. *Biochim. Biophys. Acta - Biomembr.* 1663(1–2), 117–126. doi: 10.1016/j.bbmem.2004.02.010